Search for a narrow baryonic state decaying to pK_S^0 and $\overline{p}K_S^0$ in deep inelastic scattering at HERA

ZEUS Collaboration

H. Abramowicz [y,31], I. Abt [t], L. Adamczyk [h], M. Adamus [ae], S. Antonelli [b], V. Aushev [q], O. Behnke [j], U. Behrens [j], A. Bertolin [v], S. Bhadra [ag], I. Bloch [k], E.G. Boos [o], I. Brock [c], N.H. Brook [ac], R. Brugnera [w], A. Bruni [a], P.J. Bussey [l], A. Caldwell [t], M. Capua [e], C.D. Catterall [ag], J. Chwastowski [g], J. Ciborowski [ad,33], R. Ciesielski [j,16], A.M. Cooper-Sarkar [u], M. Corradi [a,11], R.K. Dementiev [s], R.C.E. Devenish [u], S. Dusini [v], B. Foster [m,23], G. Gach [h], E. Gallo [m,24], A. Garfagnini [w], A. Geiser [j], A. Gizhko [j], L.K. Gladilin [s], Yu.A. Golubkov [s], G. Grzelak [ad], M. Guzik [h], C. Gwenlan [u], W. Hain [j], O. Hlushchenko [q], D. Hochman [af], R. Hori [n], Z.A. Ibrahim [f], Y. Iga [x], M. Ishitsuka [z], F. Januschek [j,17], N.Z. Jomhari [f], I. Kadenko [q], S. Kananov [y], U. Karshon [af], P. Kaur [d,12], D. Kisielewska [h], R. Klanner [m], U. Klein [j,18], I.A. Korzhavina [s], A. Kotański [i], U. Kötz [j], N. Kovalchuk [m], H. Kowalski [j], B. Krupa [g], O. Kuprash [j,19], M. Kuze [z], B.B. Levchenko [s], A. Levy [y], S. Limentani [w], M. Lisovyi [j,20], E. Lobodzinska [j], B. Löhr [j], E. Lohrmann [m], A. Longhin [v,30], D. Lontkovskyi [j], O.Yu. Lukina [s], I. Makarenko [j], J. Malka [j], A. Mastroberardino [e], F. Mohamad Idris [f,14], N. Mohammad Nasir [f], V. Myronenko [j,21], K. Nagano [n], T. Nobe [z], R.J. Nowak [ad], Yu. Onishchuk [q], E. Paul [c], W. Perlański [ad,34], N.S. Pokrovskiy [o], A. Polini [a], M. Przybycień [h], P. Roloff [j,22], M. Ruspa [ab], D.H. Saxon [l], M. Schioppa [e], U. Schneekloth [j], T. Schörner-Sadenius [j], L.M. Shcheglova [s], R. Shevchenko [q,27,28], O. Shkola [q], Yu. Shyrma [p], I. Singh [d,13], I.O. Skillicorn [l], W. Słomiński [i,15], A. Solano [aa], L. Stanco [v], N. Stefaniuk [j], A. Stern [y], P. Stopa [g], J. Sztuk-Dambietz [m,17], E. Tassi [e], K. Tokushuku [n,25], J. Tomaszewska [ad,35], T. Tsurugai [r], M. Turcato [m,17], O. Turkot [j,21], T. Tymieniecka [ae], A. Verbytskyi [t], W.A.T. Wan Abdullah [f], K. Wichmann [j,21], M. Wing [ac,*,32], S. Yamada [n], Y. Yamazaki [n,26], N. Zakharchuk [q,29], A.F. Żarnecki [ad], L. Zawiejski [g], O. Zenaiev [j], B.O. Zhautykov [o], D.S. Zotkin [s]

[a] *INFN Bologna, Bologna, Italy* [1]
[b] *University and INFN Bologna, Bologna, Italy* [1]
[c] *Physikalisches Institut der Universität Bonn, Bonn, Germany* [2]
[d] *Panjab University, Department of Physics, Chandigarh, India*
[e] *Calabria University, Physics Department and INFN, Cosenza, Italy* [1]
[f] *National Centre for Particle Physics, Universiti Malaya, 50603 Kuala Lumpur, Malaysia* [3]
[g] *The Henryk Niewodniczanski Institute of Nuclear Physics, Polish Academy of Sciences, Krakow, Poland* [4]
[h] *AGH–University of Science and Technology, Faculty of Physics and Applied Computer Science, Krakow, Poland* [4]
[i] *Department of Physics, Jagiellonian University, Krakow, Poland*
[j] *Deutsches Elektronen-Synchrotron DESY, Hamburg, Germany*
[k] *Deutsches Elektronen-Synchrotron DESY, Zeuthen, Germany*
[l] *School of Physics and Astronomy, University of Glasgow, Glasgow, United Kingdom* [5]
[m] *Hamburg University, Institute of Experimental Physics, Hamburg, Germany* [6]
[n] *Institute of Particle and Nuclear Studies, KEK, Tsukuba, Japan* [7]
[o] *Institute of Physics and Technology of Ministry of Education and Science of Kazakhstan, Almaty, Kazakhstan*
[p] *Institute for Nuclear Research, National Academy of Sciences, Kyiv, Ukraine*
[q] *Department of Nuclear Physics, National Taras Shevchenko University of Kyiv, Kyiv, Ukraine*
[r] *Meiji Gakuin University, Faculty of General Education, Yokohama, Japan* [7]
[s] *Lomonosov Moscow State University, Skobeltsyn Institute of Nuclear Physics, Moscow, Russia* [8]

[t] *Max-Planck-Institut für Physik, München, Germany*

[u] *Department of Physics, University of Oxford, Oxford, United Kingdom* [5]

[v] *INFN Padova, Padova, Italy* [1]

[w] *Dipartimento di Fisica e Astronomia dell' Università and INFN, Padova, Italy* [1]

[x] *Polytechnic University, Tokyo, Japan* [7]

[y] *Raymond and Beverly Sackler Faculty of Exact Sciences, School of Physics, Tel Aviv University, Tel Aviv, Israel* [9]

[z] *Department of Physics, Tokyo Institute of Technology, Tokyo, Japan* [7]

[aa] *Università di Torino and INFN, Torino, Italy* [1]

[ab] *Università del Piemonte Orientale, Novara, and INFN, Torino, Italy* [1]

[ac] *Physics and Astronomy Department, University College London, London, United Kingdom* [5]

[ad] *Faculty of Physics, University of Warsaw, Warsaw, Poland*

[ae] *National Centre for Nuclear Research, Warsaw, Poland*

[af] *Department of Particle Physics and Astrophysics, Weizmann Institute, Rehovot, Israel*

[ag] *Department of Physics, York University, Ontario, M3J 1P3, Canada* [10]

ARTICLE INFO

ABSTRACT

A search for a narrow baryonic state in the pK_S^0 and $\overline{p}K_S^0$ system has been performed in ep collisions at HERA with the ZEUS detector using an integrated luminosity of 358 pb^{-1} taken in 2003–2007. The search was performed with deep inelastic scattering events at an ep centre-of-mass energy of 318 GeV for exchanged photon virtuality, Q^2, between 20 and 100 GeV^2. Contrary to evidence presented for such a state around 1.52 GeV in a previous ZEUS analysis using a sample of 121 pb^{-1} taken in 1996–2000, no resonance peak was found in the $p(\overline{p})K_S^0$ invariant-mass distribution in the range 1.45–1.7 GeV. Upper limits on the production cross section are set.

* Corresponding author.
  E-mail address: m.wing@ucl.ac.uk (M. Wing).

1. Introduction

The observation of a narrow baryon resonance with a mass of ≈ 1.53 GeV, reported first by the LEPS experiment in 2003 [1,2] in the missing-mass distribution for γA collisions, generated considerable theoretical and experimental interest. Such a baryon would be manifestly exotic because of its decay into a K^+ and a neutron, which is impossible for a three-quark state but could be explained as a bound state of five quarks i.e. a pentaquark state. A narrow baryonic resonance close to the observed mass had previously been predicted in the chiral soliton model [3] and named Θ^+ with quark configuration $uudd\overline{s}$. Many experimental groups have looked for this state via various production processes in the decay modes nK^+ or $pK_S^0(\overline{p}K_S^0)$. Some experiments confirmed the signal while others refuted it. Several reviews [4–8] have been published on the subject.

The HERA accelerator collided electrons[1] at $E_e = 27.5$ GeV with protons at $E_p = 820$ or 920 GeV. The ZEUS experiment reported evidence for a peak structure in the pK_S^0 mass distribution[2] in deep inelastic scattering (DIS) data, consistent with a Θ^+. The data were taken between 1996 and 2000 (HERA I) and correspond to an integrated luminosity of 121 pb^{-1} [9]. The H1 Collaboration presented mass distributions in a similar kinematic region [10], but did not find any structure and presented an upper limit. However, this limit did not unambiguously exclude the ZEUS signal.

Recently, interest in pentaquark states has arisen again with the discovery of two pentaquark candidates by the LHCb experiment at 4.38 and 4.45 GeV. They have a valence quark content of $uudc\overline{c}$ and were observed with high statistical significance [11].

To clarify the production of strange pentaquarks in DIS, a search for the Θ^+ resonance in the HERA II data (2003–2007) with an integrated luminosity of 358 pb^{-1} has been performed. The HERA II period not only provided larger statistics, but also the ZEUS tracking system was upgraded. In particular, a silicon-strip micro vertex detector (MVD) [12] located close to the beam line provided more information on the ionisation energy loss per unit length, dE/dx. This improves the selection of protons from a huge background of mainly pions.

This paper presents the result of a search at HERA II for a narrow resonance in the pK_S^0 system in the central rapidity region of high-energy ep collisions in a similar kinematic region to the previous ZEUS analysis. The sample includes both e^+p and e^-p collisions at a centre-of-mass energy of 318 GeV. The analysis was done with DIS events, requiring a visible scattered electron in the detector, at a photon virtuality, Q^2, in the range 20–100 GeV^2.

2. Experimental set-up

A detailed description of the ZEUS detector can be found elsewhere [13]. A brief outline of the components that are most relevant for this analysis is given below.

Charged particles were tracked in the central tracking detector (CTD) [14], the MVD [12] and the straw-tube tracking detector (STT) [15]. These components operated in a magnetic field of 1.43 T provided by a thin superconducting solenoid. The CTD consisted of 72 cylindrical drift-chamber layers, organised in nine superlayers covering the polar-angle[3] region $15° < \theta < 164°$. The MVD silicon tracker consisted of a barrel (BMVD) and a forward (FMVD) section. The BMVD contained three layers with two detectors in each layer and provided polar-angle coverage for tracks from 30° to 150°. The four-layer FMVD extended the polar-angle coverage in the forward region to 7°. The single-hit resolution of the MVD was 24 μm. The transverse distance of closest approach (DCA) of tracks to the nominal vertex in the X–Y plane was measured to have a resolution, averaged over the azimuthal angle, of $(46 \oplus 122/p_T)$ μm, with p_T in GeV. For CTD–MVD tracks that pass through all nine CTD superlayers, the momentum resolution was $\sigma(p_T)/p_T = 0.0029 p_T \oplus 0.0081 \oplus 0.0012/p_T$, with p_T in GeV. Both the CTD and MVD were equipped with analog read-out systems which provided dE/dx information for particle identification. The STT covered the polar-angle region $5° < \theta < 25°$.

The high-resolution uranium–scintillator calorimeter (CAL) [16] consisted of three parts: the forward (FCAL), the barrel (BCAL) and the rear (RCAL) calorimeters. Each part was subdivided transversely into towers and longitudinally into one electromagnetic section (EMC) and either one (in RCAL) or two (in BCAL and FCAL) hadronic sections (HAC). The smallest subdivision of the calorimeter was called a cell. The CAL energy resolutions, as measured under test-beam conditions, were $\sigma(E)/E = 0.18/\sqrt{E}$ for electrons and $\sigma(E)/E = 0.35/\sqrt{E}$ for hadrons, with E in GeV.

The luminosity was measured using the Bethe–Heitler reaction $ep \rightarrow e\gamma p$ by a luminosity detector which consisted of independent lead-scintillator calorimeter [17] and magnetic spectrometer [18] systems. The fractional systematic uncertainty on the measured luminosity was 2% [19].

---

[3] The ZEUS coordinate system is a right-handed Cartesian system, with the Z axis pointing in the nominal proton beam direction, referred to as the "forward direction", and the X axis pointing towards the centre of HERA. The coordinate origin is at the centre of the CTD. The pseudorapidity is defined as $\eta = -\ln\left(\tan\frac{\theta}{2}\right)$, where the polar angle, θ, is measured with respect to the Z axis.

3. Monte Carlo simulation

Samples of Monte Carlo (MC) events were generated to determine the detector acceptance in order to estimate the production cross section of a resonance state in the pK_S^0 system. The generated events were passed through the GEANT 3.21-based [20] ZEUS detector- and trigger-simulation programs [13]. They were reconstructed and analysed by the same program chain as used for real data.

Signal events were generated with the MC package RAPGAP v.3.1030 [21]. Pentaquarks were simulated by replacing $\Sigma^+(1189)$ in the particle table with a pentaquark with various masses (1.450, 1.500, 1.522, 1.540, 1.560, 1.600 and 1.650 GeV), isotropically decaying into pK^0. Events that satisfy $Q^2 > 1$ GeV^2 and $|y_{pK^0}| < 2.5$, where y_{pK^0} is the rapidity of the pK^0 system, were kept and processed in the detector simulation. Thirty million events were produced with $M = 1.522$ and $M = 1.540$ GeV, which are the peak positions of the ZEUS HERA I analysis [9] and the PDG value of 2006 [22], respectively. Fifteen million events were produced for each of the other mass points.

4. Event selection

4.1. Event sample

A three-level trigger [13,23,24] was used to select DIS events, requiring scattered electron candidates. In the offline reconstruction, the scattered electron candidates were identified from the pattern of energy deposits in the CAL [16]. The Bjorken scaling variable, x, as well as y and Q^2, were reconstructed using the double-angle method [25,26] which uses the angle of the scattered electron and the angle calculated from the remaining particles. Here, $y = Q^2/(sx)$ denotes the fraction of the incoming electron energy transferred to the proton in the proton rest frame and s is the square of the centre-of-mass energy of the ep system.

The following requirements, similar to those in the HERA I analysis, were imposed to select the events for the DIS sample:

- $20 < Q^2 < 100$ GeV^2;
- $E_{e'} > 10$ GeV, where $E_{e'}$ is the corrected energy of the scattered electron measured in the CAL;
- $38 < \delta < 60$ GeV, where $\delta = \Sigma E_i(1 - \cos\theta_i)$, E_i is the energy of the ith calorimeter cell, θ_i is its polar angle and the sum runs over all cells;
- $y_e < 0.95$, and $y_{\mathrm{JB}} > 0.04$, where y_e and y_{JB} are the y values calculated by the electron and Jacquet–Blondel (JB) method [27], respectively;
- $|Z_{\mathrm{vertex}}| < 30$ cm, where Z_{vertex} is the vertex position along the Z-axis determined from the tracks.

The requirement $Q^2 > 20$ GeV^2 was motivated by the HERA I analysis; the requirement $Q^2 < 100$ GeV^2 allows a direct comparison to the H1 limit [10].

In order to check the sensitivity of the HERA II data to resonance searches, the well-known $\Lambda_c(2286)$ baryon was searched for in the pK_S^0 mass spectrum in DIS and also in a photoproduction event sample, $Q^2 \approx 0$ GeV^2. The photoproduction events were collected from various trigger streams [28] by requiring offline that no identified electron with energy $E_{e'} > 4$ GeV and $y_e < 0.85$ was found in the CAL and by imposing a cut $0.2 < \delta/E_e < 0.85$, where E_e is the electron beam energy. The same Z_{vertex} cut was imposed as in the DIS sample.

4.2. K_S^0 selection

Neutral strange K_S^0 mesons were reconstructed from two charged tracks in the decay $K_S^0 \rightarrow \pi^+\pi^-$. The tracks were required to pass through at least three inner superlayers of the CTD, to have at least three BMVD hits out of the nominal six hits, and to have transverse momentum $p_T > 0.15$ GeV and $|\eta| < 1.75$, restricting the study to a region where the track acceptance and momentum resolution were high. In view of the huge combinatorial background, only oppositely charged pairs whose three-dimensional distance of closest approach to each other was less than 1.5 cm were considered for a vertex constraint fit. The invariant mass, $M(\pi^+\pi^-)$, was calculated assigning the π mass to both tracks. The candidate pairs were required to satisfy the following conditions:

- $\chi^2 < 5.0$, where χ^2 refers to the re-fit of K_S^0 vertex position;
- $L_{XY} > 0.5$ cm, where L_{XY} is the K_S^0 decay length in the XY plane, to eliminate a background of misidentified decays close to the primary vertex;
- $\alpha_{2D} < 0.06$ radian and $\alpha_{3D} < 0.15$ radian, where α_{2D} and α_{3D} are XY-projected and three-dimensional collinearity angles, respectively, defined as the angle between the direction from the primary vertex to the decay vertex and the momentum direction of the $\pi\pi$ system;
- $p_T(K_S^0) > 0.25$ GeV, $|\eta(K_S^0)| < 1.6$.

In addition, the following requirements were imposed to eliminate contamination from other sources:

- $M(e^+e^-) > 0.07$ GeV, where the electron mass was assigned to each track, to eliminate track pairs from photon conversions;
- $M(p\pi) > 1.121$ GeV, where the proton mass was assigned to the track with the higher momentum, to eliminate Λ contamination of the K_S^0 signal.

Fig. 1 shows the invariant-mass distribution for K_S^0 candidates. A fit with two Gaussian functions plus a constant was used. The peak position was $M(K_S^0) = 0.4972$ GeV, which is consistent with the PDG value of 0.4976 GeV [29] within the uncertainty on the momentum scale of the tracks (0.3%). The candidates with $0.482 < M(\pi^+\pi^-) < 0.512$ GeV were selected. A sample of 0.31 million events was selected with at least one K_S^0 candidate.

4.3. Proton selection and particle identification

The selection of proton or anti-proton tracks makes use of kinematic requirements and particle identification (PID). In the following, the term "proton" denotes generically both the proton (p) and the anti-proton ($\overline{p}$). The kinematic selections on the proton track were as follows:

- it passes through at least three inner superlayers of the CTD and has at least two MVD hits;
- its momentum, p_{track}, satisfies $0.2 < p_{track} < 1.5$ GeV;
- it is associated with the primary vertex;
- it is not one of the tracks from the selected K_S^0 candidate.

The proton PID was performed with the combination of the CTD and MVD dE/dx information. The dE/dx in the CTD was estimated with the truncated-mean method used in previous ZEUS analyses [30,31]. The dE/dx in the MVD was estimated by a likelihood method [28]. The measured dE/dx resolution was $\approx 10\%$ for each detector.
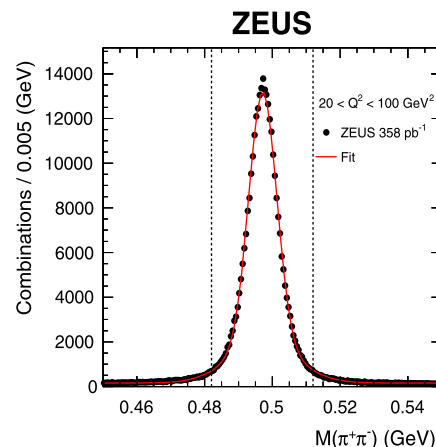

Fig. 1. The $\pi^+\pi^-$ invariant-mass distribution for $20 < Q^2 < 100$ GeV^2. The dashed lines show the mass range used for the K_S^0 selection. For illustration, the result of a fit with two Gaussian functions and constant background is shown.

The first step in selecting well measured protons required the measured dE/dx values to be within bands centred at the expectation of the respective parameterised Bethe–Bloch function [29], and to be greater than 1.15 in units of minimum-ionising particles (mips). These cut positions are indicated in Fig. 2, which shows CTD and MVD dE/dx measurements as a function of p_{track}.

The CTD and MVD dE/dx measurements for the tracks selected as protons by the other detector are shown in Figs. 2 (a) and (b), respectively. In addition to the clear proton bands, contaminations from kaons and pions are visible. In some cases, the CTD dE/dx for tracks with large energy loss is not measured due to saturation of the signal; therefore there are fewer entries at high dE/dx in the CTD plot (Fig. 2(a)).

In the second step, a likelihood-like estimator was used to select protons based on distances to the predicted Bethe–Bloch lines for proton, kaon and pion hypotheses. In cases when the CTD dE/dx was not determined because of a saturated signal, protons were selected using only the MVD dE/dx. Figs. 2 (c) and (d) show the CTD and MVD dE/dx distributions for tracks after the final selection.

The proton identification efficiency of the dE/dx selection was measured with a Λ sample, selected using the $p\pi$ invariant mass without dE/dx selection, from an extended DIS[4] sample and the photoproduction sample. The efficiency is about 80% for protons with momentum $p_{track} < 0.8$ GeV, almost linearly decreasing to 20% at $p_{track} = 1.5$ GeV, mainly due to the likelihood-like cut used to reduce the pion contamination. The identification efficiency for the protons from Λ decays integrated over p_{track} from 0.1 to 1.5 GeV is 54%. The pion-rejection factor was examined using pion tracks from K_S^0 decays. The factor is above 1000 for momenta below 1.2 GeV and decreases to 100 at 1.5 GeV.

For a direct comparison with the HERA I analysis, another event sample was prepared with protons selected using only the CTD dE/dx using the first step of logic as described above. This results in a higher integrated proton identification efficiency of 82% for protons in the Λ-decay sample, but the pion rejection factor above 0.6 GeV, where the increase in efficiency originates, is 10–100 times worse.

---

[4] In the extended DIS sample, no explicit Q^2 cut was imposed in order to keep as many Λ candidates as possible.
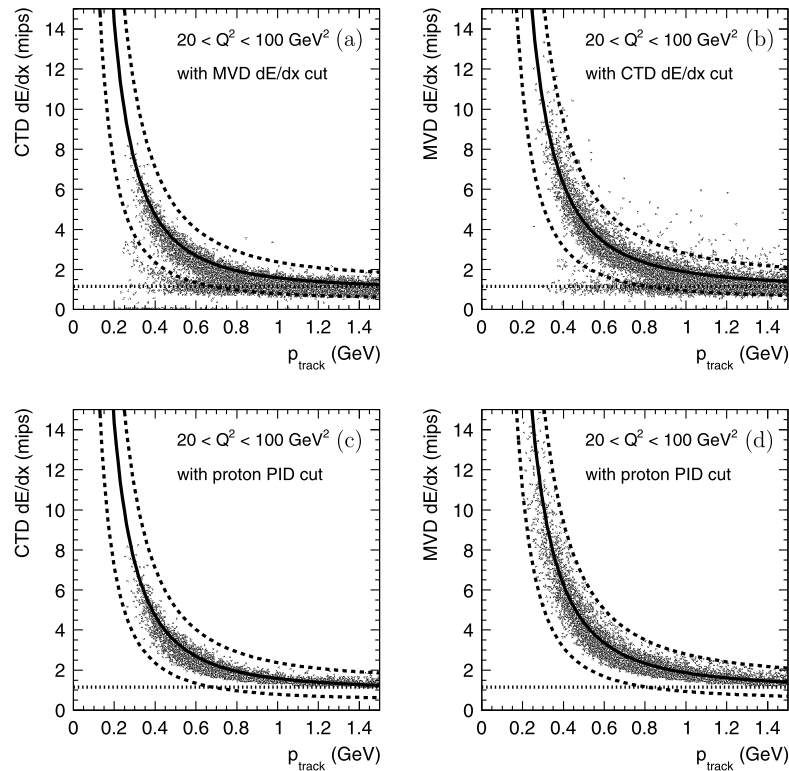
ZEUS

Fig. 2. The dE/dx distributions as a function of p_{track} for (a) the CTD and (b) the MVD for the tracks identified as protons by the dE/dx of the other detector; the distributions for (c) the CTD and (d) the MVD for the tracks finally selected as protons including tracks for which dE/dx information was only available from the MVD. The solid lines show the Bethe–Bloch values for the proton. The dashed lines indicate the limits used for the proton selection. The dotted line is drawn at 1.15 *mips*, the value used for the proton selection.

5. Results

5.1. The pK_S^0 invariant-mass distribution

The pK_S^0 invariant mass was obtained by combining proton and K_S^0 candidates selected as described above and with their masses adjusted to the PDG value [29]. The pK_S^0 candidates were selected in the kinematic region $0.5 < p_T(pK_S^0) < 3.0$ GeV and $|\eta(pK_S^0)| < 1.5$.

The pK_S^0 invariant-mass distribution in the range from 1.4 to 2.4 GeV is shown in Figs. 3 (a) and (b) for the DIS sample with $20 < Q^2 < 100$ GeV^2 and for the photoproduction sample. To suppress the combinatorial background for the $\Lambda_c(2286)$ production in the photoproduction sample, a requirement of $p_T(pK_S^0) > 0.15\,E_T^{\theta>10°}$ was imposed, where $E_T^{\theta>10°}$ is the sum of the transverse energy of the CAL cells outside a 10 degree cone from the proton-beam direction. This cut was motivated by the hard character of charm fragmentation.

A clear $\Lambda_c(2286)$ peak is observed in the photoproduction sample. It is also seen in the DIS sample with less significance. The width of the Λ_c peak is 10 MeV and is consistent with the MC simulation.

In Fig. 3(c), the pK_S^0 invariant-mass distribution is shown in the mass range from 1.4 to 1.9 GeV for the same DIS sample with finer bins. The distribution contains 3107 pK_S^0 candidates and 2833 $\overline{p}K_S^0$ candidates. The pion contamination in the proton candidates was estimated to be less than 10%. The dashed line represents the Θ^+ signal as would be observed if it had the same strength as reported in the ZEUS HERA I result. The HERA I signal is not confirmed in this analysis.

For a more direct comparison of the present to the previous ZEUS result, an analysis with CTD-only dE/dx selection and with similar cuts as in the HERA I analysis was performed. For this, no MVD information was used for the track selection. At least 40 CTD hits were required for the proton track. The result is shown in Fig. 3(d). The increase of the number of pK_S^0 candidates in Fig. 3(d), of an order of magnitude with respect to Fig. 3(c), is mainly due to the looser PID selection for the proton candidates. It is consistent with the number of candidates observed in the HERA I analysis. For this looser selection, the pion contamination in the proton candidates was estimated to be more than 50%. No peak is seen in Fig. 3(d).

5.2. Upper limits on the production cross section

Since there is no significant structure in the invariant-mass distribution, upper limits on the production cross section of a narrow pK^0 resonance were derived.

A fit was performed to the mass plot shown in Fig. 3(c) for a mass range between 1.435 and 1.9 GeV with a Gaussian function for a postulated signal and an empirical function for background of the form

$$\alpha(M - M_0)^\beta(1 + \gamma(M - M_0)),$$

where α, β and γ are parameters determined in the fit, M is the pK_S^0 mass, and M_0 is the sum of the nominal proton and K^0 masses [29].
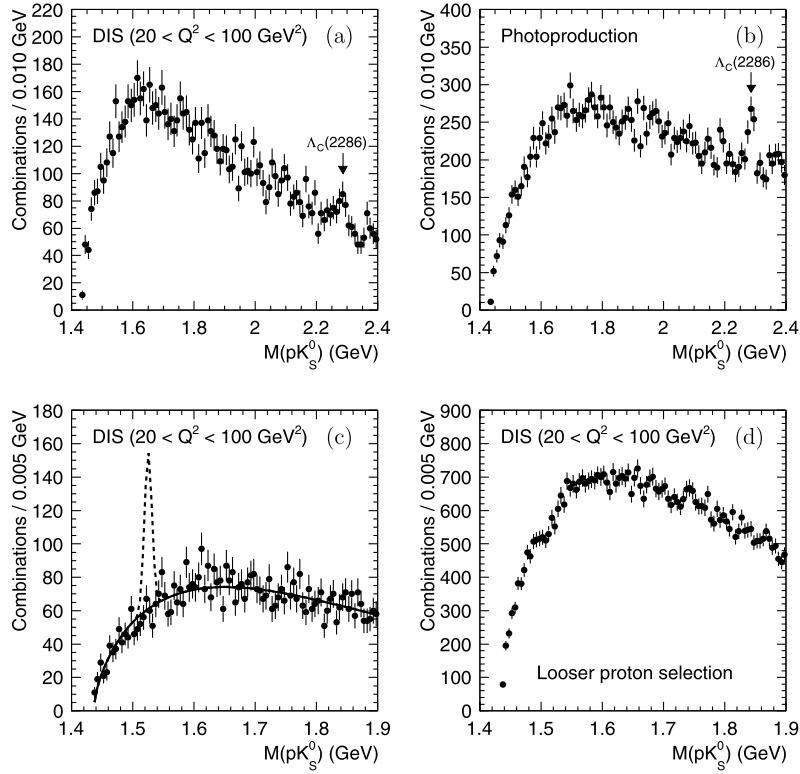
ZEUS

Fig. 3. The pK_S^0 invariant-mass distribution for (a) the DIS sample with $20 < Q^2 < 100$ GeV^2 and (b) the photoproduction sample. (c) The pK_S^0 distribution for the DIS sample with smaller bins. The solid line is the result of a fit using the background function. The dashed line represents the signal corresponding to the ZEUS HERA I result. (d) The pK_S^0 distribution as in (c) with proton PID according to the HERA I analysis.

Three options were used for the width of the Gaussian. One option was to fix it to 6.1 MeV, which is the measured value from the ZEUS HERA I analysis. In the other two options, the width was set to $1\times$ and $2\times$ the detector resolution. The resolution of the pK_S^0 invariant mass was estimated using the MC events and was 3.5 MeV in the region near 1.52 GeV and 11 MeV near 2.3 GeV. For the mass range shown in Fig. 3(c), the resolution R was parameterised with the following formula;

$$R = 0.00959\,M - 0.01111\ \text{(GeV)}. \tag{1}$$

The upper limit on the cross section at 95% confidence level (CL) was determined at the value which increases the χ^2 of the fit by 2.71 [29] with respect to the best fit.[5] At $M = 1.52$ GeV, where the peak was found in the HERA I analysis [9], the obtained upper limit is 25.8 events for a width of 6.1 MeV. For the HERA I analysis, ZEUS reported 221 ± 48 events above the background. Correcting this number of events for the luminosity and for differences in the event selection and detector efficiencies, dominated by the proton identification, the predicted number of events for this analysis is 286. In Fig. 3(c), a peak of this magnitude with resolution 6.1 MeV is shown as the dashed line above a solid curve which represents the background-only fit. Since no peak is observed at 1.52 GeV, the structure in the HERA I data is assumed to be a background fluctuation.

The cross sections were defined in the following kinematic range reflecting the region of large acceptance:

- $20 < Q^2 < 100$ GeV^2;
- $|\eta(pK^0)| < 1.5$;
- $0.5 < p_T(pK^0) < 3.0$ GeV.

The final results are shown as upper limits to the production cross section for either Θ^+ or $\overline{\Theta^+}$, multiplied by the branching ratio of $\Theta^+ \to pK^0$, i.e.

$$\sigma(\Theta) = (\sigma(ep \to e\Theta^+ X) + \sigma(ep \to e\overline{\Theta^+}X)) \times BR(\Theta^+ \to pK^0).$$

The branching ratios of the K^0 to K_S^0 transition and of the K_S^0 to $\pi^+\pi^-$ decay used in the cross-section calculation were 0.5 and 0.6895 [29] respectively.

The acceptance for the event selection was estimated using cross-section calculations from the MC samples except for the proton PID efficiency, which was determined from the Λ sample. It was assumed that the p_T and η distributions of the resonance are similar to the $\Sigma^\pm(1189)$ as generated in RAPGAP v.3.1030 [21] and that the resonance decays isotropically to pK_S^0. Since the detection efficiency depends strongly on the (p_T, η) values of the pK_S^0 system, some variations on the p_T distribution were tested as a study of the systematic uncertainty.

Systematic uncertainties on the cross section were evaluated for the following 4 components:

- uncertainty in the event selection: the acceptance corrections were recalculated by shifting selection cuts [28] and re-evaluating the upper limit on the cross section. The variance was about 10%;
- the proton PID efficiency was modified by $\pm 1\sigma$ of the measurement uncertainty. The effect was about 3% with little mass dependence;

---

[5] The best fit is obtained in the non-negative region of the signal amplitude. When the best-fit amplitude is zero, this gives a more conservative limit than at 95% CL.
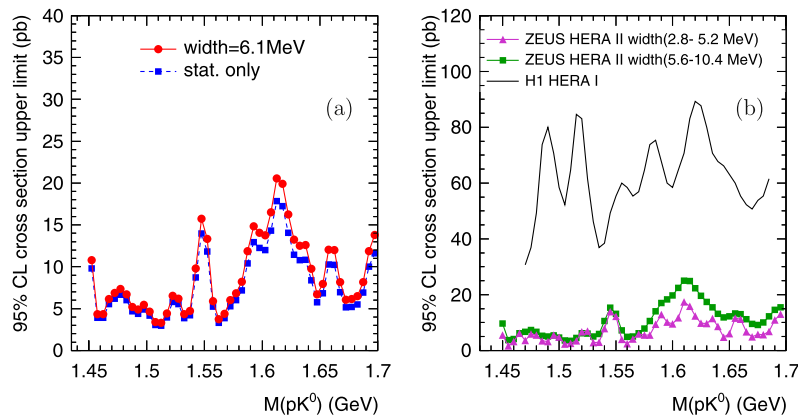
ZEUS Collaboration / Physics Letters B 759 (2016) 446–453

ZEUS

Fig. 4. The 95% CL upper limits on $\sigma(\Theta)$ for different hypotheses on the width of the observed peak; (a) 6.1 MeV and (b) the mass resolution and twice the mass resolution. In (a), the limit set by the statistical uncertainty only is also shown. In (b), the limit from the H1 result is also shown.

- uncertainty in the mass-dependent selection efficiency: the acceptance for a pK_S^0 resonance was determined using the seven MC samples for different masses as defined in Section 3. The mass dependence of the efficiency was fitted with a linear or a quadratic function to obtain the value for any given mass. The difference between the two fit functions gave a negligible contribution to the systematic uncertainty;
- model uncertainty on the p_T distribution of a pK_S^0 resonance: in this analysis, the MC samples were generated using RAP-GAP by replacing $\Sigma^{\pm}(1189)$ with resonant states at various masses (see Section 3). In the model, the p_T distribution was less steep with increasing mass. As a test, the distribution was re-scaled in order to keep the same p_T spectra for all masses. At high masses, this gave about 20% difference.

In addition, there was a 2% uncertainty on the luminosity measurement [19]. All resulting variations on the upper limit of the cross sections were added in quadrature and the upper limit was increased accordingly.

The upper limits[6] obtained on $\sigma(\Theta)$ at 95% CL are shown in Fig. 4(a) for a width of the Θ^+ of 6.1 MeV. As a reference, the limit considering only the statistical uncertainty is also shown. The limit in the region of the Θ^+ mass is below 10 pb.

In Fig. 4(b), the cross-section limits for a Θ^+ with an intrinsic width much smaller than the detector resolution (see Eq. (1)) is shown. Also shown are the limits for a Θ^+ with a width reconstructed as twice the detector resolution, which approximately corresponds to the width used for the published H1 limit. The ZEUS limit is more stringent than that obtained by H1.

6. Summary

A resonance in the $pK_S^0(\overline{p}K_S^0)$ system consistent with a Θ^+-like state has been searched for in the HERA II data collected with the ZEUS detector, exploiting the improved proton identification capability made possible by the use of the micro vertex detector. A peak at 1.52 GeV for which evidence had been observed in a previous ZEUS analysis, based on HERA I data, was not confirmed. Upper limits on the production cross section of such a resonance have been set as a function of the pK^0 mass in the

kinematic region: $0.5 < p_T(pK^0) < 3.0$ GeV, $|\eta(pK^0)| < 1.5$ and $20 < Q^2 < 100$ GeV^2.

References

[1] LEPS Collaboration, T. Nakano, et al., Phys. Rev. Lett. 91 (2003) 012002.
[2] LEPS Collaboration, T. Nakano, et al., Phys. Rev. C 79 (2009) 025210.
[3] D. Diakonov, V. Petrov, M. Polyakov, Z. Phys. A 359 (1997) 305.
[4] A.R. Dizierba, C.A. Meyer, A.P. Szczepaniak, J. Phys. Conf. Ser. 9 (2005) 192.
[5] M. Danilov, R. Mizuk, Phys. At. Nucl. 71 (2008) 605.
[6] K.H. Hicks, J. Phys. Conf. Ser. 9 (2005) 183.
[7] K.H. Hicks, Prog. Part. Nucl. Phys. 55 (2005) 647.
[8] K.H. Hicks, Eur. Phys. J. H 37 (2012) 1.
[9] ZEUS Collaboration, S. Chekanov, et al., Phys. Lett. B 591 (2004) 7.
[10] H1 Collaboration, A. Aktas, et al., Phys. Lett. B 639 (2006) 202.
[11] LHCb Collaboration, Phys. Rev. Lett. 115 (2015) 72001.
[12] A. Polini, et al., Nucl. Instrum. Methods A 581 (2007) 656.
[13] ZEUS Collaboration, in: U. Holm (Ed.), The ZEUS Detector. Status Report, DESY, 1993 (unpublished), http://www-zeus.desy.de/bluebook/bluebook.html.
[14] N. Harnew, et al., Nucl. Instrum. Methods A 279 (1989) 290;
B. Foster, et al., Nucl. Phys. B, Proc. Suppl. 32 (1993) 181;
B. Foster, et al., Nucl. Instrum. Methods A 338 (1994) 254.
[15] S. Fourletov, Nucl. Instrum. Methods A 535 (2004) 191.
[16] M. Derrick, et al., Nucl. Instrum. Methods A 309 (1991) 77;
A. Andresen, et al., Nucl. Instrum. Methods A 309 (1991) 101;
A. Caldwell, et al., Nucl. Instrum. Methods A 321 (1992) 356;
A. Bernstein, et al., Nucl. Instrum. Methods A 336 (1993) 23.
[17] J. Andruszków, et al., Preprint DESY-92-066, DESY, 1992;
ZEUS Collaboration, M. Derrick, et al., Z. Phys. C 63 (1994) 391;
J. Andruszków, et al., Acta Phys. Pol. B 32 (2001) 2025.
[18] M. Helbich, et al., Nucl. Instrum. Methods A 565 (2006) 572.
[19] L. Adamczyk, et al., Nucl. Instrum. Methods A 744 (2014) 80.
[20] R. Brun, et al., Technical Report CERN-DD/EE/84-1, CERN, 1987.
[21] H. Jung, Comput. Phys. Commun. 86 (1995) 147.
[22] Particle Data Group, W.-M. Yao, et al., J. Phys. G 33 (2006) 1.
[23] W.H. Smith, K. Tokushuku, L.W. Wiggers, in: C. Verkerk, W. Wojcik (Eds.), Proc. Computing in High-Energy Physics (CHEP), Annecy, France, CERN, Geneva, Switzerland, 1992, p. 222. Also in preprint DESY 92-150B.
[24] P.D. Allfrey, et al., Nucl. Instrum. Methods A 580 (2007) 1257.
[25] S. Bentvelsen, J. Engelen, P. Kooijman, in: W. Buchmüller, G. Ingelman (Eds.), Proc. Workshop on Physics at HERA, vol. 1, DESY, Hamburg, Germany, 1992, p. 23.

---

6 Since in the present analysis the origin of K_S^0 from K^0 or $\overline{K^0}$ cannot be distinguished, all limits are equally valid for a hypothetical narrow $p\overline{K^0}$ resonance.

[26] K.C. Höger, in: W. Buchmüller, G. Ingelman (Eds.), Proc. Workshop on Physics at HERA, vol. 1, DESY, Hamburg, Germany, 1992, p. 43.

[27] F. Jacquet, A. Blondel, in: U. Amaldi (Ed.), Proc. of the Study for an *ep* Facility for Europe, DESY, Hamburg, Germany, 1979, p. 391. Also in preprint DESY 79/48.

[28] R. Hori, KEK Report 2016-1, KEK, Tsukuba, Japan, in preparation.

[29] Particle Data Group, K.A. Olive, et al., Chin. Phys. C 38 (2014) 090001.

[30] ZEUS Collaboration, J. Breitweg, et al., Phys. Lett. B 481 (2000) 213.

[31] ZEUS Collaboration, J. Breitweg, et al., Eur. Phys. J. C 18 (2001) 625.